Available online at www.sciencedirect.com
ScienceDirect
Journal of Power Sources 158 (2006) 1140–1148
JOURNAL OF POWER SOURCES
www.elsevier.com/locate/jpowsour

Development of ultra-battery for hybrid-electric vehicle applications

L.T. Lam *, R. Louey

CSIRO Energy Technology, Bayview Avenue, Clayton South, Vic. 3169, Australia

Received 11 January 2006; received in revised form 1 March 2006; accepted 3 March 2006
Available online 2 May 2006

Abstract

Transport is one of the largest sources of human-induced greenhouse gas emissions and fossil-fuels consumption. This has lead to a growing demand for hybrid-electric vehicles (HEVs) to reduce air pollution and consumption of fossil fuels.

CSIRO Energy Technology has developed the ultra-battery, a new technology that will reduce the cost and boost the performance of batteries in HEVs. The ultra-battery is a hybrid energy-storage device, which combines an asymmetric supercapacitor, and a lead-acid battery in one unit cell, taking the best from both technologies without the need for extra electronic controls. The capacitor will enhance the power and lifespan of the lead-acid battery as it acts as a buffer in discharging and charging. Consequently, this hybrid technology is able to provide and absorb charge rapidly during vehicle acceleration and braking.

The ultra-battery has been subjected to a variety of tests. To date, results show that the discharge and charge power of the ultra-battery is ∼50% higher and its cycle-life is at least three times longer than that of the conventional lead-acid counterpart. Furthermore, the ultra-battery is able to be produced as either flooded-electrolyte or valve-regulated designs in the existing lead-acid factory and also able to reconfigure for a variety of applications, such as conventional automobile, power tool, forklift, high-power uninterruptible power supply and remote-area power supply.

The prototype ultra-batteries have been constructed and are under laboratory evaluation and field trial. The success of the ultra-battery will obviously make HEVs more affordable and widespread. This, in turn, will reduce greenhouse gas emissions in the urban environment and the consumption of limited supplies of fossil fuels.

Keywords: Asymmetric supercapacitor; Lead-acid battery; Ultra-battery; Hydrogen evolution; High-rate partial-state-of-charge duty; Sulfation; Hybrid-electric vehicles

1. Background

Transport is one of the largest sources of human-induced greenhouse gas emissions and fossil-fuels consumption. Thus, the ideal future transport should be directed towards to the use of the zero-emission, electric vehicle and/or fuel-cell vehicle, which uses alternative fuel, such as hydrogen. Since these vehicles are still under development and improvement, the low-emission and less fuel consumption, hybrid-electric vehicles (HEVs) have been developed for use during this transition time.

The present commercial HEVs consist of an internal-combustion engine (ICE) and an electric motor, which is powered by an energy-storage pack. Both the ICE and electric motor can be connected either in series (e.g., Toyota Prius) or in parallel (e.g., Honda Insight) configuration. With such an arrangement, the ICE can be operated most of the time at very efficient speed (i.e., cruise conditions) in terms of fuel consumption and exhaust emissions, and the power required for acceleration is provided by the energy-storage pack. There are several types of HEVs, namely, 'micro-hybrid', 'mild hybrid', 'full (or power-assist) hybrid' and 'hybrid with pure-electric driving range'. In the last version of HEV, the vehicle requires to be operated by the pure electrical energy from the energy-storage pack for several mileages in urban area. In order to meet the respective demand, the energy-storage pack must provide sufficient energy and power for stop-start and idle-stop in micro- or mild hybrid (e.g., 0.5–1 kWh or 9–15 kW), additional energy and power for power assist in full hybrid (e.g., 1–3 kWh or 20–60 kW) and extra energy for pure-electric driving range hybrid (10–20 kWh or 50–100 kW). The energy storage in the above HEVs operates continuously at high rates and under partial state-of-charge (HRPSoC) mode. High-rate discharge is necessary for engine

* Corresponding author. Tel.: +61 3 9545 8401; fax: +61 3 9545 8403.
E-mail address: lan.lam@det.csiro.au (L.T. Lam).

0378-7753/$ – see front matter © 2006 Elsevier B.V. All rights reserved.
doi:10.1016/j.jpowsour.2006.03.022

cranking and acceleration (i.e., power assist), while high-rate charge is associated with regenerative braking.

At present, candidate energy storage systems for HEV applications include valve-regulated lead-acid (VRLA), nickel-metal hydride, rechargeable lithium batteries, and supercapacitor. It is well known that supercapacitor can provide high power, but low energy and, therefore, for HEV applications, this technology should be used in conjunction with other batteries. It is obvious that VRLA battery has the great advantages of low initial (capital) cost, well established manufacturing, distributing network and high recycling efficiency over the other competitive technologies. Nevertheless, the running cost of this battery is expensive because of the short service life. The VRLA battery under HEV applications must be operated within 30–70% SoC. This is because the battery cannot deliver the required cranking current when the SoC is below 30%. On the other hand, the battery cannot accept charge efficiently either from regenerative braking or from engine charging when SoC is above 70%. In addition, it is well documented [1–5] that under such applications, the VRLA battery fails prematurely due to the sulfation of the negative plates. The negative plates suffer from a progressive build-up of 'hard' lead sulfate on the surface, i.e., lead sulfate which is difficult to recharge. The accumulation of lead sulfate reduces markedly the effective surface-area to such extent that the plate can no longer deliver and accept the power required by engine cranking, acceleration, and regenerative braking. The key factors responsible for such failure are both the high-rate discharge and the high-rate charge. High-rate discharge causes a compact layer of lead sulfate formed on the surface of the negative plate. On the other hand, high-rate charge promotes an early evolution of hydrogen and, therefore, reduces the charging efficiency of the plate. Since the VRLA batteries experience short service-life in HEVs, at present, most of the HEVs use the more expensive nickel-metal hydride batteries as its electrical power source.

Based upon the above failure mechanism, several approaches can be taken to improve the cycleability of the VRLA battery under HEV duty, such as:

(i) localization of charging current on plate surface by superimposing the battery with high-frequency pulses [6];
(ii) reduction of plate thickness and addition of carbon at high level to minimize the uneven distribution of lead sulfate within the cross-section of the negative plate [7–9].

Although the cycle-life of the VRLA battery with the above modifications has been improved significantly, the degree of improvement still does not reach the desirable target required by the HEVs (e.g., lifetime of the vehicle) as the battery still failed because of negative-plate sulfation. The way to further improve the cycle-life of VRLA battery is to connect the battery with a supercapacitor in parallel. With such configuration, the supercapacitor will provide the high power (or current) for engine cranking and will adsorb the high power from regenerative braking. This, in turn, will protect the battery being discharged and charged at the high rates. Therefore, the battery life is enhanced. Since the operational voltage of the supercapacitor is greatly different to that of the VRLA battery, an electronic control is required to regulate the current flow between the two devices. Unfortunately, this arrangement will add significantly extra complexity and cost to the system. Accordingly, CSIRO has developed an advanced ultra-battery, superseding the conventional supercapacitor/lead-acid battery system.

2. Ultra-battery

2.1. Structure of ultra-battery

The ultra-battery, in fact, is a hybrid energy-storage device, which combines an asymmetric supercapacity and a lead-acid battery in one unit cell, without extra electronic control. The schematic structure of the ultra-battery is shown in Fig. 1. A lead-acid cell comprises one lead-dioxide positive plate and one sponge lead negative plate. On the other hand, an asymmetric supercapacitor composes of one lead-dioxide positive plate and one carbon-based negative plate (i.e., capacitor electrode). Since the positive plates in the lead-acid cell and the asymmetric supercapacitor have the common composition, these two devices can be integrated into one unit cell by connecting internally the capacitor electrode and the lead-acid negative plate in parallel. Both electrodes now share the same lead-acid positive plate. With this design, the total discharge or charge current of the combined negative plate is composed of two components. One is the capacitor current. Other is the lead-acid negative plate current. Accordingly, the capacitor electrode can now act as a buffer to share the discharge and charge currents with the lead-acid negative plate and thus, prevents it being discharged and charged at the high rates.

Having said that, it does not mean that the ultra-battery can be easily achieved by just inserting any capacitor electrodes into a lead-acid battery. This is because there is a difference in the operational potential range between the capacitor electrode and the lead-acid negative plate.

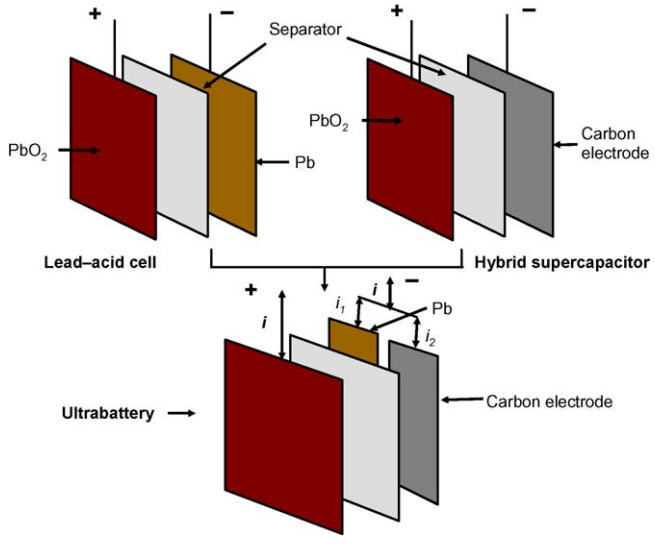

Fig. 1. Configuration of ultra-battery.

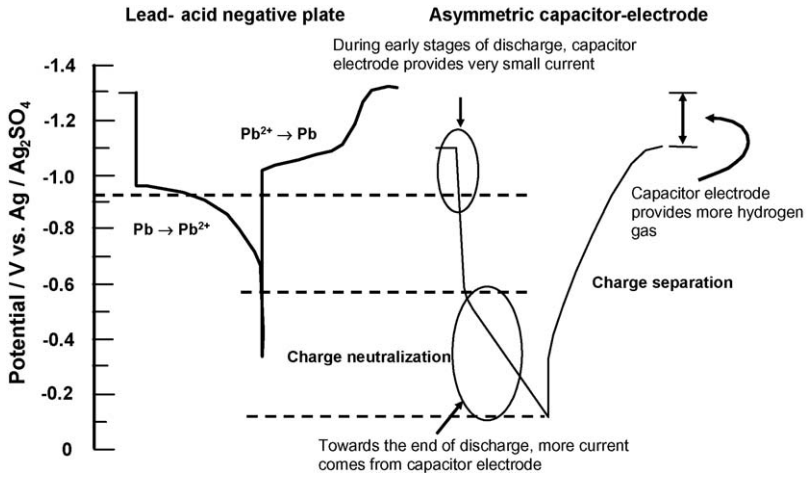

Fig. 2. Operational potentials of a lead-acid negative plate and a carbon-based capacitor electrode during discharge and charge.

2.2. Differences in operational potential

The operational potentials of lead-acid negative plate and a carbon-based capacitor electrode during discharge and charge are shown in Fig. 2. During discharge, the sponge lead starts to convert to lead sulfate at the potential about −0.98 V. During charge, the lead sulfate starts to convert back to sponge lead at potential less than −1.0 V. On the other hand, during discharge, the charge neutralization on the capacitor electrode occurs at potential greater than −0.5 V and during charge, the charge separation occurs at potential less than −0.3 V. Now, if both electrodes are connected in parallel and discharged. The combined negative-plate potential will maintain at −0.98 V initially where the sponge lead is converted to lead sulfate. This means that during early stages of discharge, the current mainly comes from the lead-acid negative plate and only little from the capacitor electrode owing to its higher charge-neutralization potential (i.e., −0.5 V). Obviously, this is not the desirable condition. As the discharge progresses, more current will comes from capacitor electrode through charge neutralization when the combined negative-plate potential increases to a value greater than −0.5 V. This is because little reaction occurs at the lead-acid negative electrode. During charging, the current will flow to the capacitor electrode first and then to the lead-acid negative plate. Toward the end of charge, however, the capacitor electrode will evolve significant hydrogen gas than the lead negative-plate because its potential now is shifted to a more negative value than it should be (Fig. 2).

2.3. Modification of capacitor material

From the above discussion, it is clear that the cycle-life of the battery will not be improved by simply connecting the capacitor electrodes with the lead negative-plates because of two reasons. First, the capacitor electrode cannot share the current with the lead negative plate during the early stages of discharge. Second, more hydrogen gassing will occur from the capacitor electrodes towards the end of charging and this will cause the electrolyte dry-out of the battery. Thus, in order to make the ultra-battery become workable, significant effort should be paid to the modification of the capacitor electrode so that it has:

(i) similar working potential to that of the lead-acid negative plate;
(ii) low hydrogen gassing rate;
(iii) higher capacity to share the current with the lead-acid negative plate at least for 30 s;
(iv) long cycle-life;
(v) sufficient mechanical strength and ability to produce in the existing lead-acid factory;
(vi) low cost.

In addition, the ultra-battery should be redesigned so that it can accommodate the capacitor electrode without causing major increase in battery weight. In this paper, the performance of capacitor electrode alone and the ultra-battery is reported.

3. Performance of capacitor electrode

3.1. Hydrogen-gassing rate

Valve-regulated lead-acid (VRLA) batteries which require no water maintenance are increasingly replacing conventional, flooded batteries in many applications. Since VRLA batteries with absorptive glass-microfibre (AGM) separators employ lower volumes of sulfuric acid solution than their flooded equivalents, the former technology generally operates under ‘acid-starved’ conditions. Thus, any excessive loss of water through, for example, poor cell design and/or incorrect operation, will limit both the capacity and the life of the battery.

Typically, a VRLA battery can suffer water loss via the following routes:

(i) gas leakage, through inadequate sealing of the battery container;
(ii) gas leakage, through the battery container itself;
(iii) gas escape via the venting valve during charging;
(iv) heavy grid corrosion.

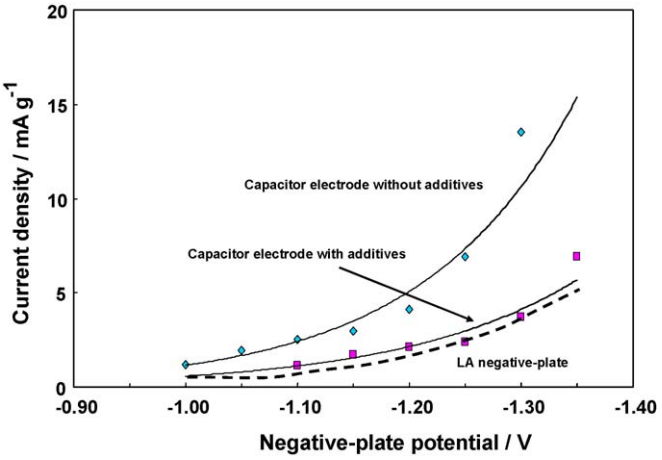

Fig. 3. Hydrogen-evolution rates on the lead-acid negative plate and the capacitor electrodes with or without additives.

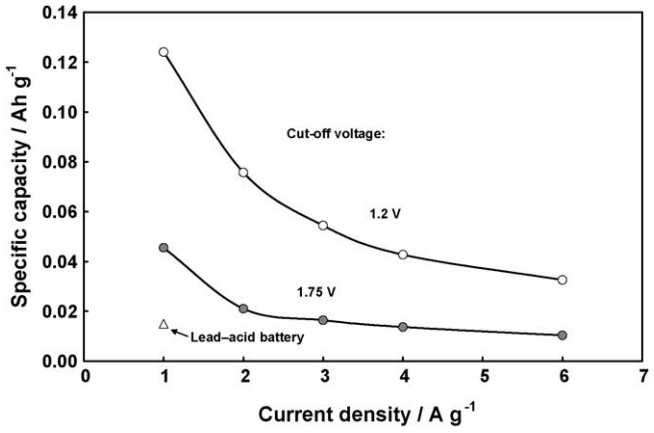

Fig. 4. Capacity performance of the capacitor electrode at different current densities and cut-off voltages.

Obviously, water loss caused by (i) and (ii) is due to inadequate battery manufacturing and/or design. By contrast, water loss through (iii) and (iv) is unavoidable, owing to the inherent characteristics of VRLA batteries. Oxygen and hydrogen evolution occur as side reactions during the charging process of lead-acid batteries. In a VRLA battery, however, the oxygen evolved from the positive plates diffuses through the pores of the separators or the headspace of the container to the negative plates where it is reduced back to water. By contrast, the hydrogen evolved from the negative plates cannot be oxidized (or rather can only be oxidized at a very low rate) back to water at the positive plates. Thus, any hydrogen emission during charging will translate to a permanent loss of the water from the battery. Accordingly, the hydrogen-evolution rate on the capacitor electrode should be examined in order to ensure that it could be integrated with the VRLA battery without causing significant water loss.

The hydrogen gassing on the full-charge lead-acid negative plate and capacitor electrodes with or without additives was conducted in 1.280 relative density H_2SO_4 under 21 °C using potentiostat technique. The potential of each electrode was set at a given value for a given time until the delivered current reached the stable value. Since both electrodes were fully charged, the delivered current was considered as the result of the hydrogen-evolution reaction. The capacitor electrodes were made from a mixture of carbon black, activated carbon and binder with or without additives. The hydrogen-evolution currents on the lead-acid negative plate and capacitor electrodes at different potentials are shown in Fig. 3. The hydrogen-evolution current increases with the decrease of potential, irrespective of electrode types. At a given potential, clearly, the hydrogen evolves more on the capacitor electrode without additives than on lead negative plate. Nevertheless, the hydrogen-evolution rate reduces significantly to the levels close to that of lead negative electrode when the capacitor electrode was doped with additives. This indicates that both electrodes can now be connected in parallel without causing substantial electrolyte dry-out under high rates partial-state-of-charge operation.

3.2. Capacity and cycle-life performance

As mentioned in Section 2.3, the capacitor electrode should have high capacity and long cycle-life in order to share the current with the lead-acid negative plate, and to enhance the life of the combined plate. Accordingly, the capacity and cycling performance of the capacitor electrode were first examined. The capacity performance of the capacitor electrode at different current densities and cut-off voltages is shown in Fig. 4. It can be seen that the specific capacity of the electrode decreases with the increase of discharge current density. Nevertheless, the capacity decreases at current density greater than 2 A g^{-1} is not significant for electrode with the cut-off voltage at 1.75 V than at 1.2 V. It needs to note here that the discharge current density of 1 A g^{-1} is close to the cranking current density of a lead-acid battery. At this current, the specific capacity of the lead-acid battery at the cut-off voltage of 1.2 V is 0.015 Ah g^{-1}, which is much lower than that of the supercapacitor. This indicates that the supercapacitor gives higher capacity than the lead-acid battery at high current discharge.

The cycling performance of the capacitor electrode at different discharge current densities is shown in Fig. 5. Clearly, the capacity of the electrode is fairy stable at 3 and 4 A g^{-1}, but increases gradually with cycling when the current density

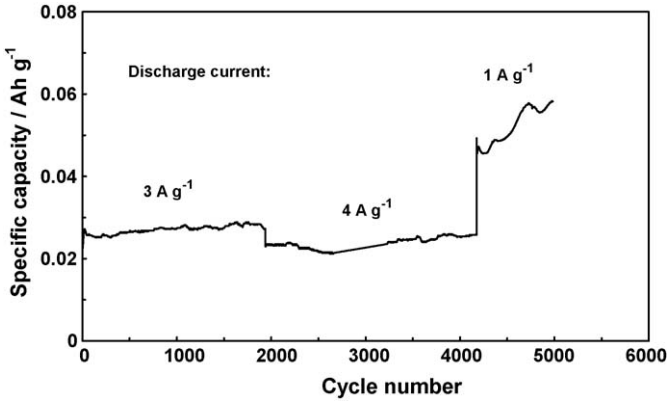

Fig. 5. Cycling performance of the capacitor electrode at different discharge current densities.

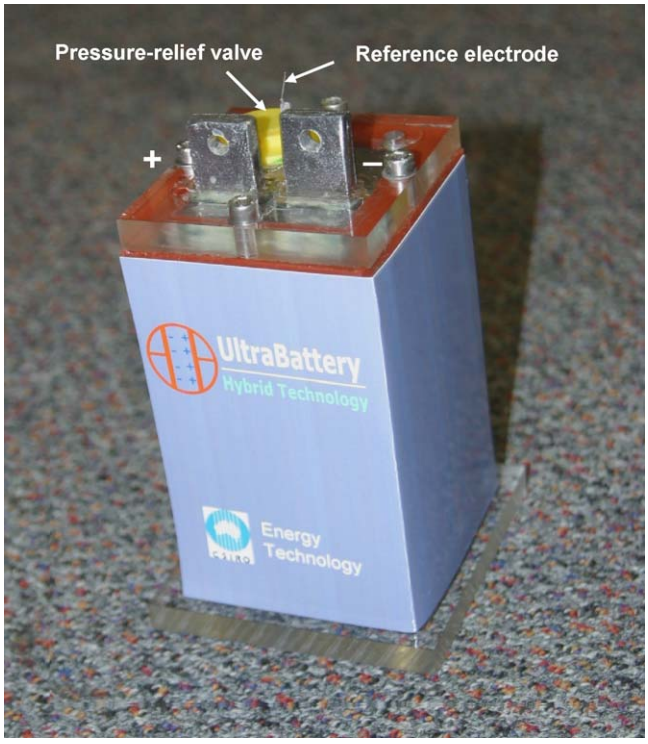

Fig. 6. Photograph of an ultra-cell.

is reduced to 2 A g^{-1}. It is well known that the capacity of the lead-acid battery will decrease rapidly within 80 cycles when the battery is cycled repetitively at the reserved-capacity rate [10]. The current densities used for testing the capacitor electrode here are much severer than the reserved-capacity rate, namely, 2–4 A g^{-1} versus 0.05–0.1 A g^{-1}. Nevertheless, the electrode has undergone up to 5000 cycles and is still in a healthy condition.

To date, the capacitor electrode has been modified to such an extent that the hydrogen evolution on this electrode during charging has been reduced significantly to the level close to that of the lead-acid negative plate. In addition, this electrode can also provide high capacity and significantly long cycle-life. Therefore, it is expected that the power and the cycle-life of the ultra-battery will be enhanced when this capacitor electrode is used.

4. Performance of ultra-battery

The VRLA ultra-cell used in this study is shown in Fig. 6. The cell was fitted with one-way pressure-relief valve and a silver/silver sulfate reference electrode for the measurement of positive- and negative-plate potentials during discharge and charge cycling [11].

4.1. Power

One of the most important requirements for a battery used in HEV is the power performance during vehicle acceleration and regenerative braking. Fig. 7 shows the discharge and charge power behaviour of the control cell (i.e., cell without supercapacitor) and the ultra-cell. The discharge power of the cell decreases, while the regenerative power increases with the increase of the depth-of-discharge (DoD), respective of either control cell or ultra-cell. At a given depth-of-discharge, however, the discharge and charge power of the ultra-cell are greater than those of the control counterpart. The discharge and charge power have been improved by ~50% and ~60%, respectively. This indicates that the ultra-cell can be operated at a wider depth-of-discharge window, but still can provide and receive similar power levels to that of the conventional VRLA battery.

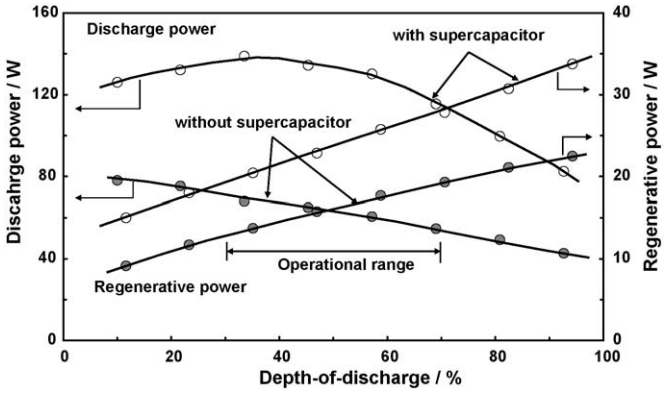

Fig. 7. Power performance of the control cell and ultra-cell.

4.2. Cycling performance

The evaluation of battery cycle-life is the time-consumed process. In the interests of expediency, the test programme in this study is divided into two main parts, namely, screening test component and cycle-life test component. This is because the differences in battery performance, if any, will appear quicker under the screening test. For cycle-life test, two profiles were used. One is to evaluate the endurance of battery in hybrid buses and other is in hybrid-electric vehicles.

4.2.1. Screening test

The simplified discharge and charge profile used to evaluate the control cell and ultra-cell is shown in Fig. 8. The profile

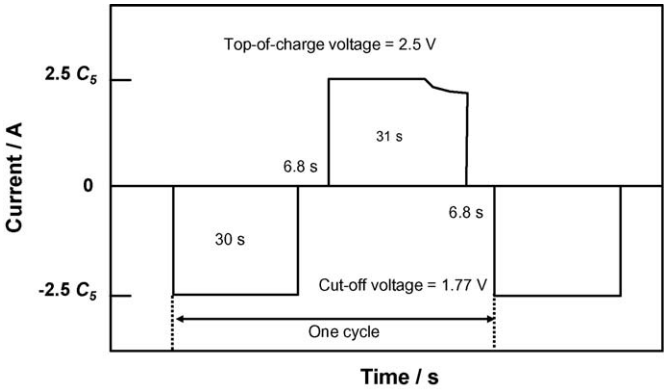

Fig. 8. Simplified discharge and charge profile.

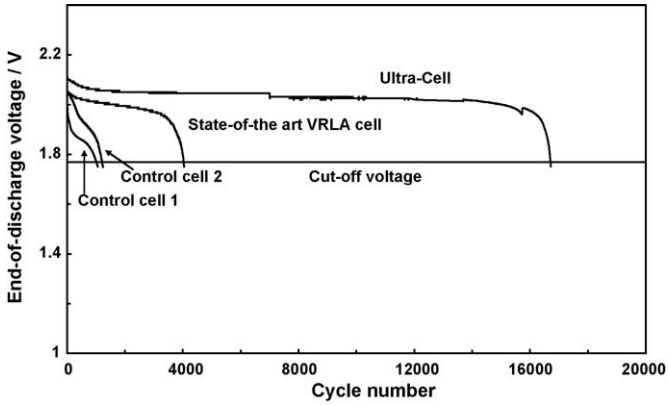

Fig. 9. Cycling performance of the control cells and ultra-cell under simplified discharge and charge profile.

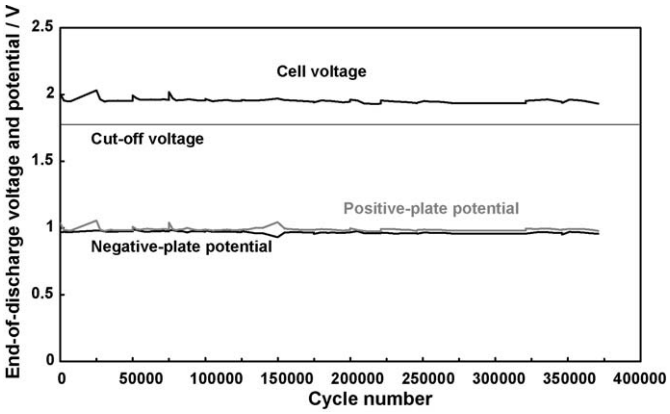

Fig. 10. Cycling performance of ultra-cell under simplified hybrid-bus profile.

composes of a discharge at $2.5C_5$ A for 30 s and a charge at a constant voltage of 2.5 V with maximum current of $2.5C_5$ A for 31 s. There are two-rest time of 6.8 s each in between discharge and charge or charge and discharge. The cells were subjected repetitively to this profile at 40 °C until the voltage of each cell reached 1.77 V.

The performance of the two control cells is fairy consistent, namely, the end-of-discharge voltage (EoDV) of both cells reached the cut-off value at ∼1300 and 1500 cycles, respectively (Fig. 9). On the other hand, the cell using negative plates doped with carbon black and graphite completed ∼4000 cycles, which is about 2.7 times longer than that of the control counterparts. As expected, the ultra-cell achieved ∼17,000 cycles, which is much longer than the control cells and cell doped carbon and graphite in the negative plates.

4.2.2. Cycle-life test—simplified hybrid-bus profile

The simplified hybrid-bus profile is selected to evaluate the cell performance [12]. The profile is similar to the screening test profile, except that the duration of discharge and charge is reduced to 8 and 8.4 s, respectively. The cells were subjected to this profile repetitively for 12,500 cycles, followed by a full charge at a constant voltage of 2.5 V with a maximum current of $0.1C_5$ A for 8 h. After charged, the cells were subjected to a further set of 12,500 cycles. The test was terminated when the cell voltage reached the cut-off value of 1.77 V. It should be note here that with this profile, every 12,500 cycles obtained at the laboratory test is equivalent to 1 month in the field trial. Nakayama et al reported that their VRLA batteries using negative plates doped with conductive fibre achieved 312,500 cycles under the above test profile [12].

In this study, however, the ultra-cell was subjected to the above profile repetitively for sets of 25,000 cycles, instead of 12,500 cycles in the interests of expediency. The performance of the ultra-cell is shown in Fig. 10. It can be seen that the EoDV and the end-of-discharge potentials (EoDPs) of positive and negative plates are very stable during cycling. The cell has now performed up to 370,000 cycles, and is still in a healthy condition.

4.2.3. EUCAR power-assist profile test

The European (EUCAR) power-assist profile is selected in this study because this profile can simulate the driving conditions of the HEVs [13]. The duration of the profile is short, namely, ∼2 min (Fig. 11). The profile comprises a discharge to simulate the power assist (i.e., $5C_2$ A, $C_2 = 2$ h capacity), a rest period and a recharge with three stepped currents (i.e., $4.5C_2$ A, $2.5C_2$ A and C_2 A, respectively) to simulate the charging from regenerative braking and engine. During discharge, the battery must deliver a current of $5C_2$ A and, accordingly, the voltage of the battery will fall to its lowest level. The top-of-charge voltage during each stepped-current charging of the power-assist profile was regulated at 2.45 V.

Initially, the 2 h capacity (i.e., C_2) was determined, i.e., the cell was discharged at the 2 h rate until the voltage reached 1.67 V. Recharge was conducted at a constant voltage of 2.45 V with a maximum current of $0.5C_2$ A until the 10% overcharge was achieved. The above discharge and charge was repeated for few cycles until stable capacity was reached. The cell was then placed in the water bath maintained at 40 °C. The cycle-life of the cell was conducted as follows:

(i) discharged the cell at $0.5C_2$ A to 60% SoC (i.e., 60% of the initial 2 h capacity);

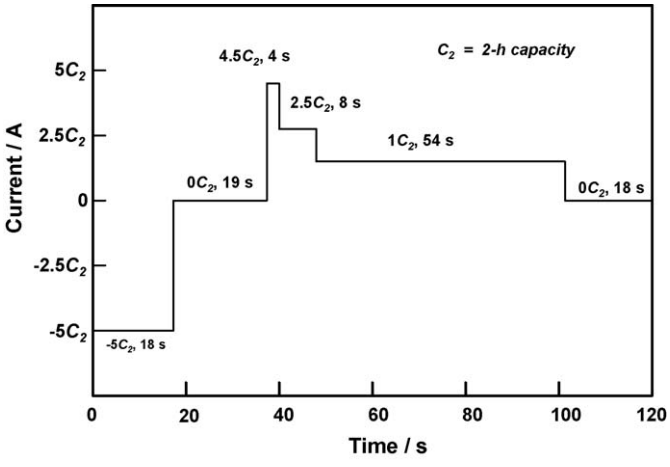

Fig. 11. EUCAR power-assist profile.

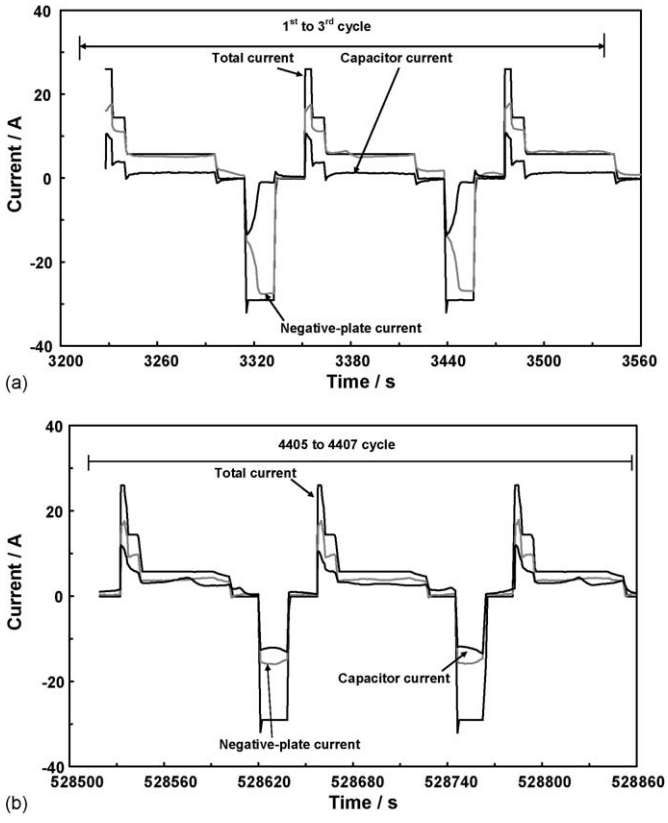

Fig. 12. Current shared between the lead-acid negative plate and the capacitor electrode during each power-assist profile: (a) during 1–6 cycles; (b) during 4405–4410 cycles.

(ii) subjected the cell to the power-assist profile repetitively for 10,000 cycles;
(iii) recharged at constant voltage of 2.45 V with maximum current of $0.5C_2$ A for 20 h;
(iv) determined the 2 h capacity of the cell, followed by a full charge (i.e., 10% overcharge);
(v) repeated steps (i)–(iv) until the measured capacity at the final 10,000 cycles reached 50% of the initial value or the cell voltage during the power-assist cycling fell below 1.4 V.

Two control cells and three ultra-cells (i.e., UB1 to UB3) were prepared and subjected to the above test profile. Fig. 12 shows the current shared between the capacitor electrodes and the lead-acid negative plates during each power-assist profile. This current measurement was conducted on the parallel connection of the asymmetric supercapacitor and the lead-acid cell through the voltage across the two shunts. One is connected in series with the negative terminal of the asymmetric supercapacitor. Other is connected to the negative terminal of the lead-acid cell. It can be seen that the charge current of the capacitor displays similar shape since the beginning of cycling (Fig. 12(a) and (b)). On the other hand, the discharge current delivered by the capacitor behaves differently with cycling. The current shows a rapid increase initially and then decays afterwards during the 18 s discharge of the EUCAR power-assist profile (Fig. 12(a)). This is because the capacitor was discharged completely when the two

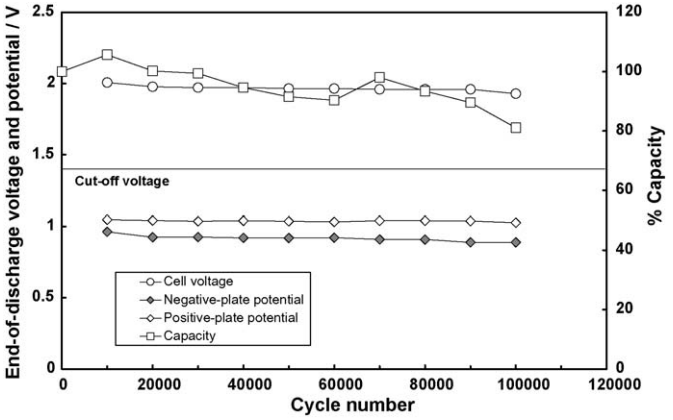

Fig. 13. Change in end-of-discharge voltage (EoDV), end-of-discharge potential (EoDP) of the positive and negative plates, together with the measured 2 h capacity after each set of 10,000 power-assist cycles of an ultra-cell (UB2).

parallel-connected cells was brought down to 60% SoC prior to the cycling. As cycling progresses, the discharge current of the capacitor becomes stable throughout the 18 s discharge period and the capacitor now can share nearly half of the total current (Fig. 12(b)). This indicates that the lead-acid negative plate can be protected being discharged and charged at full rates.

An example of the changes in EoDV and EoDPs of the positive and negative plates, together of the measured 2 h capacity after each 10,000 power-assist cycles of an ultra-cell (UB2) is shown in Fig. 13. Clearly, the EoDV of the cell, EoDP of the positive and negative plates maintain very constant during cycling. On the other hand, the capacity of the cell shows a gradual decrease with cycling. To date, this cell has achieved 100,000 cycles and is still in a healthy condition. The performance of control cells and ultra-cells under EUCAR power-assist cycling is summarized in Fig. 14. The control cells completed ~34,000–38,000 cycles, while the ultra-cells are still on test.

The ultra-battery technology has been patented and the prototype batteries are under construction and evaluation [14,15]. These batteries have a 5 h capacity of 30 Ah and are produced using the existing B24 size containers at Furukawa plant (Fig. 15).

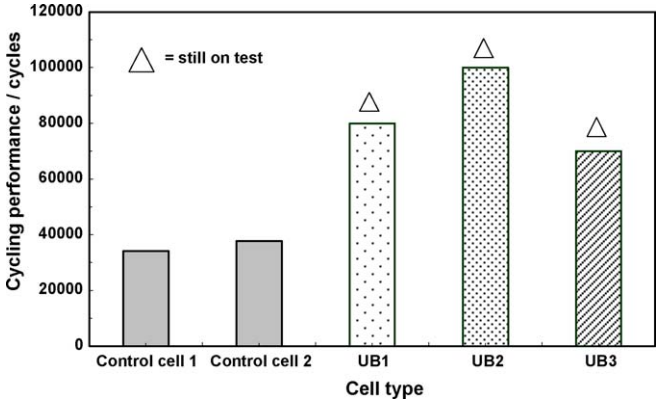

Fig. 14. Cycle-life performance of the control cells and ultra-cells.

Fig. 15. Prototype VRLA ultra-battery produced at Furukawa Battery Co. Ltd.

5. Cost of different energy-storage technologies

Obviously, it is of interest to compare the cost of ultra-battery with the other technologies for the micro-hybrid applications (Table 1). The data of lithium-ion, nickel-metal hydride and ultracapacitor-lead-acid battery systems are given by Anderman at the Ninth European Lead Battery Conference (9ELBC), Berlin, Germany [16]. It can be seen that the costs of lithium-ion and nickel-metal hydride systems are US$ 1020 and 660, respectively. On the other hand, the supercapacitor and VRLA battery system costs US$ 1070, which is even more expensive than the lithium-ion counterpart. Nevertheless, the VRLA battery in this system is only US$ 70 and the rest is due to costs of supercapacitor and dc/dc converter. For our ultra-battery, it is estimated at about US$ 200, but this cost will be reduced significantly to around the US$ 120 mark when it is mass produced.

Table 1
Costs of different energy-storage technologies for micro-hybrid vehicle applications

Energy-storage system	System weight (kg)	Cost (US$)
1 kWh lithium ion	34	1000
500 Wh, 12 V battery		20
Total		1020
750 Wh NiMH	55	620
500 Wh SLI battery		20
12 V starter battery		20
Total		660
Supercapacitor/VRLA battery		70
80 Wh supercapacitor		800
1 kWh VRLA battery		70
3 kW dc/dc converter		180
500 Wh, 12 V battery		20
Total		1070
1 kWh ultra-battery	55	200
500 Wh, 12 V battery		20
Total		220

6. Conclusions

CSIRO Energy Technology has developed the ultra-battery, a new technology that will reduce the cost and boost the performance of batteries in HEVs. This battery is a hybrid energy-storage device, which combines an asymmetric supercapacitor, and a lead-acid battery in one unit cell, taking the best from both technologies without the need for extra electronic controls. The ultra-battery has been evaluated under a variety of tests and the results show that this advanced battery has the following features and benefits:

- Greater power and significant improvement in service life.
- Able to be produced in smaller size, with sufficient power to drive the bigger engine capacity in conventional automobiles.
- Applicable to mild and full HEVs with greatly reduced cost compared with the existing nickel–nickel-metal hydride technology.
- Reconfigurable for a variety of applications (i.e., power tool, high-power uninterruptible power supply and remote-area power supply).
- Able to produce in the existing lead-acid factory.
- Low cost.

References

[1] L.T. Lam, C.G. Phyland, D.A.J. Rand, A.J. Urban, ALABC Project C2.0, Novel Technique to Ensure Battery Reliability in 42-V PowerNets for New-generation Automobiles, Progress Report: August 2001–January 2002, CSIRO Energy Technology, Investigation Report ET/IR480R, March 2002, 19 pp.
[2] L.T. Lam, N.P. Haigh, C.G. Phyland, D.A.J. Rand, A.J. Urban, ALABC Project C 2.0, Novel Technique to Ensure Battery Reliability in 42-V PowerNets for New-generation Automobiles, Final Report: August 2001–November 2002, CSIRO Energy Technology, Investigation Report ET/IR561R, December 2002, 39 pp.
[3] L.T. Lam, N.P. Haigh, C.G. Phyland, T.D. Huynh, D.A.J. Rand, ALABC Project C 2.0, Novel Technique to Ensure Battery Reliability in 42-V PowerNets for New-generation Automobiles, Extended Report: January–April 2003, CSIRO Energy Technology, Investigation Report ET/IR604R, May 2003, 23 pp.
[4] A.F. Hollenkamp, W.G.A. Baldsing, S. Lau, O.V. Lim, R.H. Newnham, D.A.J. Rand, J.M. Rosalie, D.G. Vella, L.H. Vu, ALABC Project N1.2, Overcoming Negative-plate Capacity Loss in VRLA Batteries Cycled Under Partial State-of-charge Duty, Final Report: July 2000–June 2002, CSIRO Energy Technology, Investigation Report ET/IR491R, June 2002, 47 pp.
[5] L.T. Lam, N.P. Haigh, C.G. Phyland, A.J. Urban, J. Power Sources 133 (2004) 126–134.
[6] L.T. Lam, N.P. Haigh, C.G. Phyland, T.D. Huynh, J. Power Sources 144 (2005) 552–559.
[7] L.T. Lam, N.P. Haigh, O.V. Lim, T. Lwin, C.G. Phyland, D.G. Vella, ALABC Project TE-1, Influence of trace elements, plate-processing conditions, and electrolyte concentration on the performance of valve-regulated lead-acid batteries at high temperatures and under high-rate partial-state-of-charge operation, Final Report: August 2003–July 2005, CSIRO Energy Technology, Investigation Report ET/IR809R, July 2005, 43 pp.
[8] F. Trinidad, J. Valenciano, I. Dyson, A.F. Hollenkamp, H. Ozgun, ALABC Project N4.2, Optimisation of the negative active material and PSoC cycle life of VRLA batteries for 42V mild hybrid applications, Final Report: July 2003–June 2005. Issued: September 2005, 117 pp.
[9] S. Osumi, M. Shiomi, K. Nakayama, K. Sawai, T. Funato, M. Watanabe, H. Wada, ALABC Project N5.2, Development of additives in neg-

ative active material to suppress sulfation during high-rate-partial-state of charge operation, Final Report: July 2003–June 2005, Issued: May 2005, 51 pp.
[10] L.T. Lam, H. Ozgun, O.V. Lim, J.A. Hamilton, L.H. Vu, D.G. Vella, D.A.J. Rand, J. Power Sources 53 (1995) 215–228.
[11] P. Ruetschi, J. Power Sources 116 (2003) 53–60.
[12] Y. Nakayama, E. Hojo, T. Koike, J. Power Sources 124 (2003) 551–558.
[13] F. Trinidad, C. Gimeno, J. Gutierrez, R. Ruiz, J. Sainz, J. Valenciano, J. Power Sources 116 (2003) 128–140.
[14] Australian Patent 905086 (2003).
[15] International Patent PCT/AU/001262 (2004).
[16] M. Anderman, Analysis of an ultracapacitor/VRLA hybrid power source for hybrid vehicles, in: Proceedings of the Ninth European Lead Battery Conference, Berlin, Germany, September 21–24, 2004.